

# A Real-time Dynamic Deformable Model for Soft Tissue Simulation using Adaptive Mesh Refinement

Huynh Quang Huy Viet, Yoshinori Tsujino, Hironori Yamashita, Yasufumi Takama, Hiromi T.Tanaka

Department of Human and Computer Intelligence, Ritsumeikan University

**In this paper we propose a new method for real-time modeling of soft objects, of which high resolutions dynamically adapt to the regions of high deformation. In order to reduce the computational cost in comparison with the previous methods we use the bisection refinement algorithm. The experimental results show the effectiveness of the proposed method.**

**Keywords:** Tetrahedral Meshes, Cracks, Adaptive Refinement, Binary Subdivision, Binary Simplification, Mass-Spring Model, Deformable Objects

## 1. Introduction

The real-time interactive models and simulations of behaviors of deformable objects play important roles in several fields such as robotics, computer graphics, CAD, computer aided surgery. In mesh-based representation of a given object, the preciseness in representing is related to the number of its cells which is called the resolution of the mesh. To control the computational time for modeling, the concept of multi-resolution model have been introduced [1–6]. Multi-resolution models are the models that represent objects and their behaviors at different levels of resolution. The main advantage of a multi-resolution model is in reducing the computational cost by way of reducing the data for modeling in any place that low resolution representation is appropriate.

Throughout a simulation, to obtain a realistic behavior, different regions of interest in the model of an object might require to be represented by a high resolution and hence need to be refined. The regions of interest have been classified as: regions of contact, regions of high deformation and regions of high curvature.

There are two approaches that have been used for refinement a mesh: the approach based on the known Delaunay algorithm [7] and the approach based on the longest-side bisection algorithms [8–12]. The second approach guarantees the generation of good-quality of surface triangulation and volume tetrahedralization with *linear time* complexity, comparing to the computational cost of  $O(N\log N)$  of that of the first approach.

In [3, 6] the models for real time deformation of soft objects with high resolution at regions of contact have been proposed, the Delaunay algorithms have been used for mesh refinement. However in the paper, adaptive models with high resolution representation at regions of high

deformation have not been investigated.

In this paper we propose a new method for real-time adaptive modeling of soft object with high resolutions for regions of high deformation based on strain energy. In order to reduce the computational cost in comparison with the previous methods we use the bisection refinement algorithm proposed in the preceding researches [8–10]. The experimental results show the effectiveness of the proposed method.

The remainder of the article is organized as follows: next section reviews the bisection refinement algorithm. Section 3 presents the method for adaptive modeling the deformation of a soft object with high resolution for regions of high deformation. Section 4 describes experimental results and discussions. Finally section 5 is devoted for conclusions and future works.

## 2. Bisection Refinement-based Tetrahedral Adaptive Mesh

We first give an over view of the tetrahedral adaptive mesh, which had been developed for multi-resolution volume modeling [10], as shown in Figure 1. The mesh generation algorithm recursively bisects tetrahedra elements by increasing the number of mesh nodes according to local volume properties, such as the field value and its gradient, i.e., the orientation and curvatures of isosurfaces, until the entire volume has been approximated within a specified level of view-invariant accuracy.

### 2.1. Recursive Binary Subdivision

The algorithm for constructing the hierarchical representation is based on a stepwise refinement of an initially given grid. Given accuracy criteria, binary subdivision of the parent tetrahedron  $T_p$  occurs when the accuracy criteria, *Acc\_Thresh*, is violated for any six edges of  $T_p$ . The subdivision of  $T_p$  into two left and right tetrahedron,  $T_l$  and  $T_r$ , occurs by the creation of a new node,  $M$ , the middle point of the base edge  $E(= \overline{P_1P_2})$  of maximum length, followed by initialization of  $M$  with the local properties, such as the field value and its gradient, i.e., the orientation, curvatures of an isosurface containing  $M$ . Then, the violation of *Acc\_Thresh* is recursively evaluated for each  $T_l$  and  $T_r$  independently.

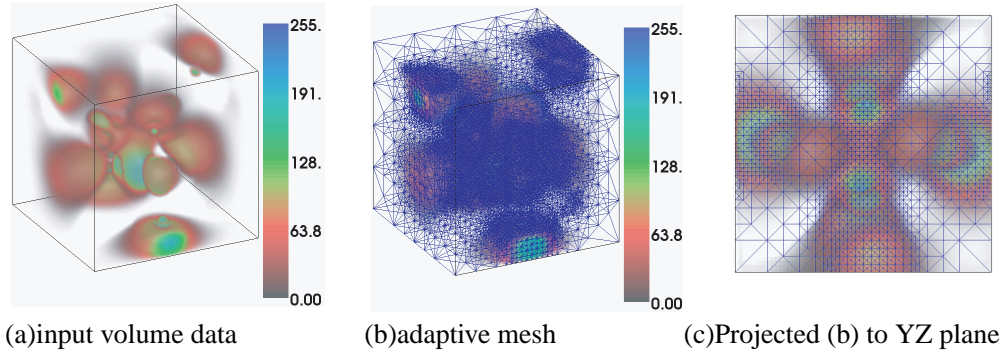


**Fig. 1.** Tetrahedral adaptive mesh of volume data

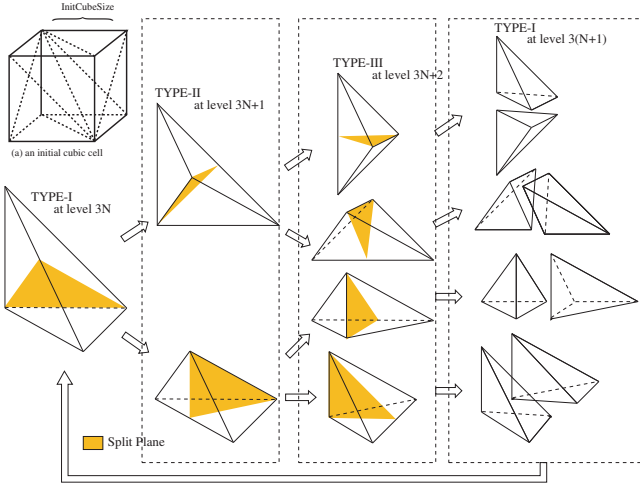


**Fig. 2.** Cyclic subdivision of a tetrahedron into TYPE-I, TYPE-II and TYPE-III primitives

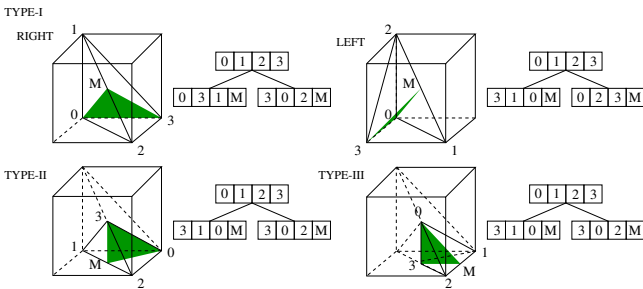


**Fig. 3.** Recursive definition of  $T_l$  and  $T_r$  for three primitives

## 2.2. Tetrahedral Primitives

In recursive binary-subdivision, only three tetrahedral primitives including mirror-symmetry, TYPE-I, TYPE-II, TYPE-III, are generated at level  $3N, 3N+1, 3N+2$ , respectively, as shown in Fig. 2. Fig. 3 shows recursive definitions of  $T_l$  and  $T_r$  using the parent node  $(P_0, P_1, P_2, P_3)$  and  $M$  for TYPE-I, TYPE-II, TYPE-III. As Fig. 2 shows three successive subdivision of a parent tetrahedron  $T_p$  of TYPE-I at level  $3N$ , generate the same type of great-ground children of TYPE-I cyclically

at level  $3(N+1)$  with each edge length and its volume decreased by 2 and by 8 respectively.

Face shapes of TYPE-I, TYPE-II, TYPE-III are either an isosceles triangle or a right triangle. With ratio of maxim to minimum edge length  $\sqrt{3}$  at TYPE-I,  $2\sqrt{2}/\sqrt{3}$  at TYPE-II, 2 at TYPE-III, respectively. This binary tetrahedrization using the middle points thus satisfies the equiangular requirement. Another advantage of the binary tetrahedrization is that it provides a more continuous level of volume approximation, because a tree with fewer descendants has more levels of approximation for a given range of volume variation.

## 2.3. Crack Handling for Discontinuities

The major problem with adaptive subdivision techniques is that *cracks*, i.e., discontinuities, may arise if each tetrahedron is subdivided independently.

When there is a large field variation near the initial grid element, a crack may be formed along the boundary between the grid elements. This crack is caused by the unilateral subdivision of a grid element on one side of the large field variation. In order to avoid cracks between adjacent tetrahedron, we had developed a parallel algorithm that detects discontinuities and preserves continuities without the formation of cracks. This crack handling algorithm collects field discontinuity information by recursively expanding the neighborhood of adjacent tetrahedra until the discontinuities are observed. The boundary reached by this recursive expansion defines the 3D region of reference for a grid element. This local definition of a *bounded* region of reference allows each grid element to be subdivided independently. Thus, the parallel computation of hierarchical tetrahedrization with no cracks is performed in bounded time and space.

## 3. Adaptive Volumetric Mass-Spring Model

The mass-spring models comprising mass node, springs and dampers for representing deformation are widely applied because of the effectiveness in computation and the simplicity in implementation. However, in the large mass-spring models computation for deforma-

tion which covers the entire nodes of the object makes the real-time simulation difficult. Therefore combining locally refinement methods with mass-spring models have been utilized to reduce the cost of computation. This section presents the model that allows the automatic adaptation of the resolution at regions of high deformation.

### 3.1. Regions of High Deformation

Throughout a simulation process, it is necessary to refine different regions in order to have high precision for representing realistic behaviours, and to simplify the refined regions for fast computation of the simulation when the high precision is not required any more. The regions of interest has been classified as: Regions of contact, regions of high deformation and regions of high curvature. In this research we focus on the regions of high deformation due to bending in a deformation process. In a deformation process of an object modeled by a tetrahedral mesh, the regions of high deformation can be characterized by the density of strain energy:

$$D_{density} = \frac{\frac{1}{2} \sum_{i=1}^6 k_i (l_i - L_i)}{V} \dots \dots \dots (1)$$

here,  $k, l, L$  are spring stiffness current lengths and initial lengths. In other words, the regions of high deformation are tetrahedrons of which the density of strain energy  $D_{density}$  exceed a given criterion  $Th$ .

### 3.2. Bisection Refinement

We use the bisection algorithm mentioned in the previous section for refining the regions of high deformation. In the bisection algorithm a tetrahedron is subdivided into two smaller tetrahedrons at the point of the base edge. The algorithm is easy to implement and moreover its computation complexity is linear time. The main problem with the bisection refinement is discontinuities or cracks. The crack handling algorithm is presented in detail in [9, 10, 13].

### 3.3. The Parameters of Mass-Spring System

While refining a mass-spring mesh it is necessary to supplement extra masses, springs and dampers. In order to guarantee the consistency of the behavior at different resolutions, a methodology for assigning mass values, spring and damper parameters have been proposed in [6, 14]. Given a material density  $D$  the mass value  $m_i$  of each vertex  $i$  according to the volume  $V_j$  of its adjacent tetrahedron  $T_j$  is as follows:

$$m = \frac{D \sum_j V_j}{4}, \dots \dots \dots (2)$$

Let  $E$  be the material elastic modulus, if  $L_{init}$  is a resting length of the spring/edge of a tetrahedral, the stiffness value of edge  $e$  is obtained by summing all of the contributions of the tetrahedron  $V_j$  incident on  $e$ :

$$k = \frac{E \sum_j V_j}{L_{init}^2} \dots \dots \dots (3)$$

The damper value of an edge  $e$  linking a mass  $m_i$  with mass  $m_j$  is given as follows [6]:

$$c = \frac{2\sqrt{k(m_i + m_j)}}{L_{init}} \dots \dots \dots (4)$$

where  $k$  is the stiffness value of the edge  $e$ .

In the binary subdivision, every tetrahedron is subdivided at the middle point of its base edge, i.e., the longest edge, we can associate a base edge  $L(n)$  after the  $n$ th subdivision with the bounding volume  $V(n)$  of a group of tetrahedra sharing  $L(n)$ , which we call a diamond, as shown in Fig.4. If  $L(n)$  is a diagonal edge inside a cubic cell at level  $n(=3N)$  then  $V(n)$  is the cubic cell itself consisting of six tetrahedra sharing  $L(n)$ . If  $L(n)$  is a diagonal edge on a bounding face shared by adjacent cubic cell, then  $V(n)$  consists of 4 tetrahedron, two from its own cubic cell and other two from the adjacent cell. If  $L(n)$  is parallel to one of the X, Y, Z coordinate axes, then  $V(n)$  consists of eight tetrahedron from four adjacent cells sharing  $L(n)$ .

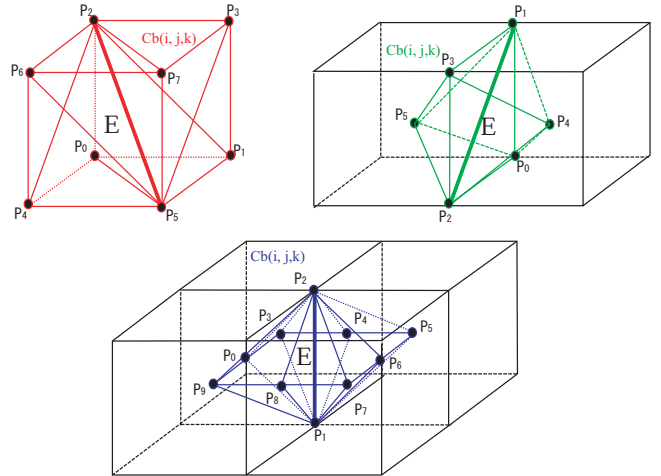


**Fig. 4.** The bounding volume of E at level  $n(=3N)$ ,  $n+1(=3N+1)$ , and  $n+2(=3N+2)$

Therefore at a division level  $n$ , the stiffness parameter  $k(n)$  and damper parameter  $c(n)$  of an edge  $e$  linking a mass  $m_i$  with mass  $m_j$  can be expressed as,

$$k(n) = \frac{EV(n)}{L(n)^2} \dots \dots \dots (5)$$

$$c(n) = \frac{2\sqrt{k(n)(m_i + m_j)}}{L(n)} \dots \dots \dots (6)$$

$$CubeSize(n) = 2^{-\lfloor \frac{n}{3} \rfloor} \times intCubeSize. \dots \dots (7)$$

$$L(n) = A \times CubeSize(n). \dots \dots (8)$$

$$V(n) = B \times CubeSize(n)^3. \dots \dots (9)$$

where

$$A = \begin{cases} \sqrt{3} & \text{if } (n \bmod 3) == 0 \\ \sqrt{2} & \text{if } (n \bmod 3) == 1 \\ 1 & \text{otherwise} \end{cases} \dots (10)$$

$$B = \begin{cases} 1 & \text{if } (n \bmod 3) == 0 \\ \frac{1}{3} & \text{otherwise} \end{cases} \dots (11)$$

### 3.4. Binary Simplification

During a simulation, a region of high deformation can become a region of low deformation and hence it should be restored to its original resolution in order to reduce the computation cost. When an edge of a subdivided tetrahedron becomes shorter to a given criterion  $T_s$ , we perform a combination procedure to simplify the refined mesh. The refined tetrahedrons are gradually combined to original tetrahedrons as showed in the figure 5. To guarantee the consistency of the behavior at different resolutions, the mass, spring and damper parameters are calculated by the formulas mentioned in the previous section.

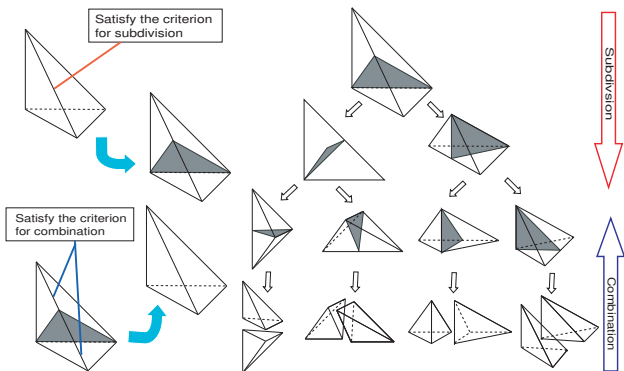


Fig. 5. Refinement and simplification processes

## 4. Experimental Results

We build the system as showed in Fig.6 to implement the proposed method. The handling of the virtual object in 3D virtual space is performed by using the haptic interface device Phantom. The visual is represented in a X3D display screen.

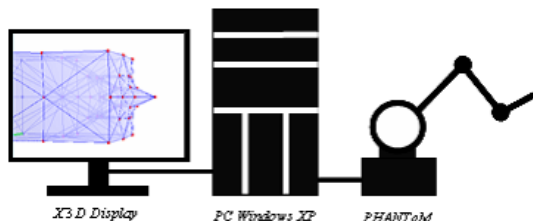


Fig. 6. System Diagram

We examine the deformation of the object in an adaptive resolution model in comparison with the low and high

resolution models. We apply the proposed adaptive resolution model for the object which is initially modeled at the low resolution. During the deformation process, the regions of high deformation in the model are gradually refined by the bisection refinement algorithm. Visually it is quite similar to the deformed shape in the high resolution model.

### 4.1. On-the-go refinement and simplification in regions of interest

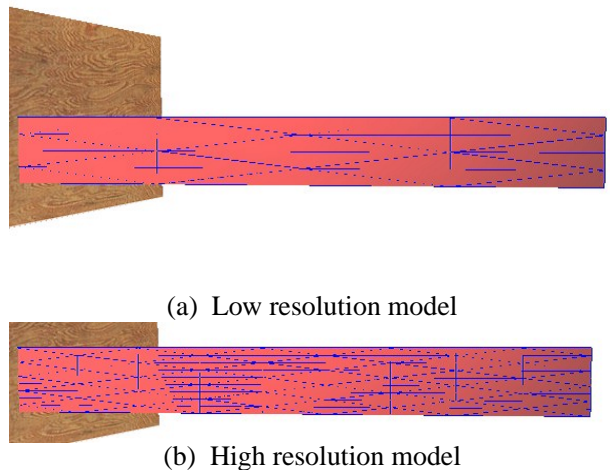


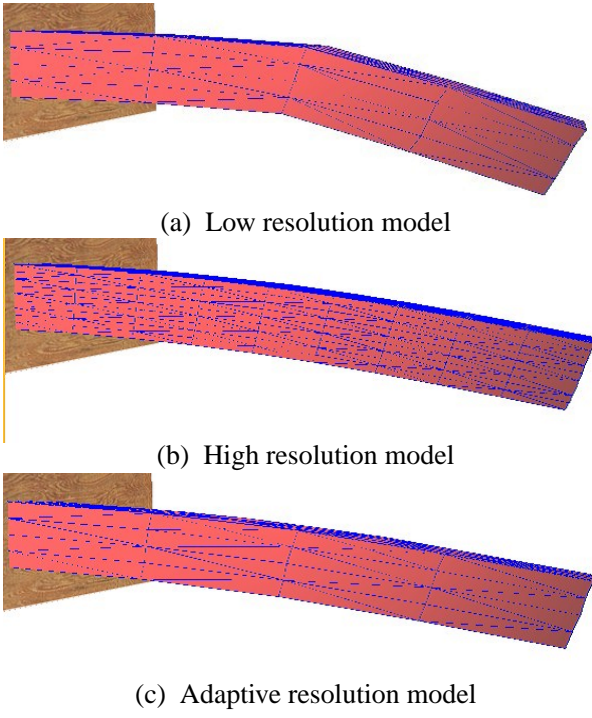
Fig. 7. The initial shape of a cuboid object.

Figure 7 shows a cuboid object modeled by tetrahedral meshes. One end of the object is fixed and the other end is free. Figure 7(a) shows a low resolution model and Fig. 7(b) shows a high resolution model. We examine the deformation of the object in an adaptive resolution model in comparison with the low and high resolution models. The object is deformed by a constant force perpendicular to the axis direction of the object at the right end, and is released to return the original shape after a given time. In the experiment the elastic modulus  $E$  is set to  $5.0 \times 10^4 [Pa]$  and the density is set to  $1.0 \times 10^2 [kg/m^3]$ .

Figure 8(a) and (b) show the deformed shape of the object in low and high resolution models. As predicted, in high resolution model the deformed shape of the object is realistic, and on the other side in low resolution model the deformed shape is rough.

We apply the proposed adaptive resolution model as mentioned in Sect.III for the object which is initially modeled at the low resolution. During the deformation process, the regions of high deformation in the model are gradually refined by the bisection refinement algorithm presented in Sect.II. In this experiment, the regions of high deformation is defined by the criterion  $T_c = 1.05$ . A tetrahedron in the regions of high deformation is refined to  $1/8$  of its initial volume. Figure 8(c) shows the deformed shape of the object in the adaptive resolution model. Visually it is quite similar to the deformed shape in the high resolution model. We almost cannot recognize the difference in the shapes.





**Fig. 8.** The deformation states in low, high and adaptive resolution model.

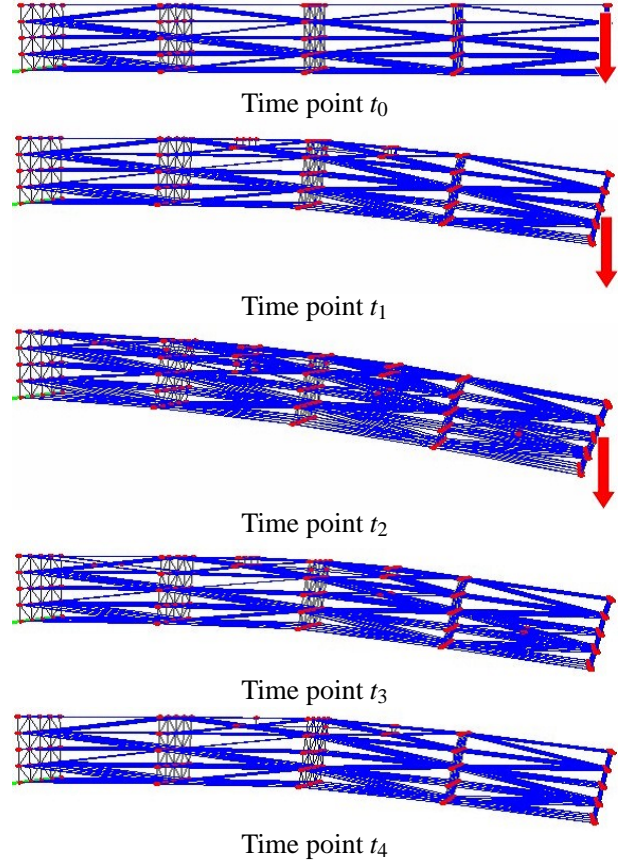
Figure 9 show the intermediate states of the deformation process in the above adaptive resolution model. The time point  $t_2$  is the time point that the object is released to return to the original shape. The mesh is gradually refined and then simplified at the regions of high deformation.

**Table 1.** The number of mesh elements

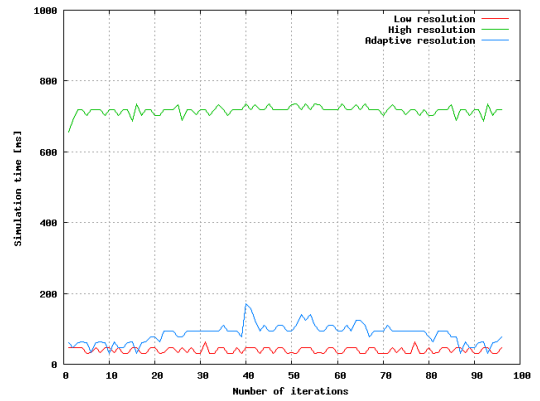
| Resolution Model | Node Number | Tetrahedron Number |
|------------------|-------------|--------------------|
| Low              | 125         | 384                |
| High             | 1000        | 4374               |
| Adaptive         | 299         | 1048               |

Table1 shows the number of nodes and tetrahedrons at the time point  $t_2$  (see Fig. 9) in the adaptive resolution model in comparison with the low and high resolution models.

Figure 10 shows diagram of the computational time per iteration for low, high and adaptive resolution model. It shows that the computational time varies among the resolution models. It stays high for the high resolution model, low for the low resolution model and is gradually increasing for the adaptive resolution model in corresponding to high deformation states. Despite the time consumption in the refinement process, the computational time of the adaptive resolution model stay quite low in comparison with that of high resolution model throughout the deformation process.



**Fig. 9.** The intermediate deformation states of the object in the adaptive resolution model.



**Fig. 10.** The comparison of computational time in low, high and adaptive models. (a) Low-resolution. (b) High-resolution. (c) Adaptive-resolution

#### 4.2. Deformation Measure For Refinement

Fig.11 shows another experiment. The object is a cuboid which fixed at the left end. We deform the object by providing a displacement for the vertex at the center of the face of the right end. Fig.11(a)(b) gives results in low and high resolutions. It is clear that in low resolution the deformation of the object is represented unfaithfully.

Fig.11(c) shows a result in adaptive resolution; the mesh is refined in the regions of high deformation defined by the expression (1). The deformed shape of the object is quite similar to that of in high resolution. The aim of this experiment is to show that we can consider a region of contact as a region of high deformation for refinement. In other words, the density of strain energy can be regarded as a general deformation measure for refinement.

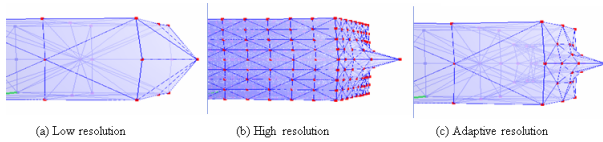


Fig. 11. Deformation in a region of contact

## 5. Conclusions

We propose a new method for real-time modeling of soft objects, of which high resolutions dynamically adapt to the regions of high deformation. In order to reduce the computational cost in comparison with the previous methods we use the bisection refinement algorithm of which computational complexity is linear time. The experiment results show the performance of the proposed method.

## References:

- [1] D. Hutchinson, M. Preston, and T. Hewitt, "Adaptive refinement for mass/spring simulations," in *Proceedings of the European workshop on Computer Animation and Simulation*, 1996, pp. 31–45.
- [2] F. Ganovelli, P. Cignoni, and R. Scopigno, "Introducing multiresolution representation in deformable modeling," in *SCCG '99 Conference Proceedings*, Budmerice (Slovakia), April 1999, pp. 149–158.
- [3] F. Ganovelli, P. Cignoni, C. Montani, and R. Scopigno, "A multiresolution model for soft objects supporting interactive cuts and lacerations," *Computer Graphics Forum*, vol. 19, no. 3, pp. 271–282, 2000.
- [4] G. Debunne, M. Desbrun, M.-P. Cani, and A. Barr, "Adaptive simulation of soft bodies in real-time," in *Computer Animation*, May 2000, pp. 133–144.
- [5] X. Wu, M. S. Downes, T. Goktekin, and F. Tendick, "Adaptive nonlinear finite elements for deformable body simulation using dynamic progressive meshes," in *Eurographics*, 2001, pp. 439–448.
- [6] C. Paloc, F. Bello, R. Kitney, and A. Darzi, "Online multiresolution volumetric mass spring model for real time soft tissue deformation," in *Proceedings of the 5th International Conference on Medical Image Computing and Computer-Assisted Intervention*, London, UK, 2002, pp. 219–226.
- [7] J. Shewchuk, "Tetrahedral mesh generation by delaunay refinement," in *Proceedings of the Fourteenth Annual Symposium on Computational Geometry*, Minneapolis, Minnesota, 1998, pp. 86–95.
- [8] H. T.Tanaka and F. Kishino, "Adaptive mesh generation for surface reconstruction: Parallel hierarchical triangulation without discontinuities," in *Proc. IEEE Conf. Computer Vision Pattern Recognition (CVPR93)*, New York City, 1993, pp. 88–94.
- [9] H. T.Tanaka, "Accuracy-based sampling and reconstruction with adaptive meshes for parallel hierarchical triangulation," *Computer Vision and Image Understanding*, vol. 61, no. 3, pp. 335–350, 1995.
- [10] H. T.Tanaka, Y. Takama, and H. Wakabayashi, "Accuracy-based sampling and reconstruction with adaptive grid for parallel hierarchical tetrahedrization," in *Proc. the 2003 Eurographics/IEEE TVCG Workshop on Volume graphics*, Tokyo, Japan, 2003, pp. 79–86.
- [11] M.-C. Rivara, "New mathematical tools and techniques for the refinement and/or improvement of unstructured triangulations," in *5th International Meshing Roundtable*, 1996, pp. 77–86.
- [12] J. M. Maubach, "Local bisection refinement for n - simplicial grids generated by reflection," *SIAM J. Scientific Computing*, vol. 16, pp. 210–227, 1995.
- [13] A. Tanaka, K. Hirota, and T. Kaneko, "Deforming and cutting operation with force sensation," *Journal of Robotics and Mechatronics*, vol. 12, no. 3, pp. 292–303, 2000.
- [14] A. V. Gelder, "Approximate simulation of elastic membranes by triangulated spring meshes," *Journal of Graphics Tools*, vol. 3, no. 2, pp. 21–42, 1998.
- [15] J. Shewchuk, *PhD thesis, Delaunay Refinement Mesh Generation*. Pittsburgh, Pennsylvania: School of Computer Science, Carnegie Mellon University, 1997.
- [16] J. Ruppert, "A delaunay refinement algorithm for quality 2-dimensional mesh generation," *Journal of Algorithms*, vol. 18, no. 3, pp. 548–585, 1995.
- [17] M. Desbrun, P. Schroder, and A. Barr, "Interactive animation of structured deformable objects," in *Graphics Interface*, 1999, pp. 1–8.
- [18] H. D. Stephane Cotin and N. Ayache, "Real-time elastic deformations of soft tissues for surgery simulation," *IEEE Transactions on Visualization and Computer Graphics*, vol. 5, no. 1, pp. 62–73, 1999.
- [19] M. Garland, "Multiresolution modeling: Survey and future opportunities," in *EUROGRAPHICS '99, State of the Art Report*, 1999, pp. 111–131.
- [20] C. Paloc, F. Bello, R. Kitney, and A. Darzi, "Virtual reality surgical training and assessment system," in *Computer Assisted Radiology and Surgery*, 2001, pp. 207–212.
- [21] J. Zhang, S. Payandeh, and J. Dill, "Haptic subdivision: An approach to defining level-of-detail in haptic rendering," in *Proceedings of the 10th Symposium on Haptic Interfaces for Virtual Environment and Teleoperator Systems*, USA, 2002, pp. 201–208.
- [22] S. Payandeh, J. Dill, and J. Zhang, "A study of level-of-detail in haptic rendering," *ACM Transactions on Applied Perception (TAP)*, vol. 2, no. 1, pp. 15–34, 2005.
- [23] Y. Choi, M. Hong, M. Choi, and M. Kim, "Adaptive surface-deformable model with shape-preserving spring," *Computer Animation and Virtual Worlds*, vol. 16, no. 1, pp. 69–83, 2005.